AIMS Mathematics, 10(8): 19750–19774.
DOI: 10.3934/math.2025881
Received: 01 May 2025
Revised: 26 June 2025
Accepted: 07 July 2025
Published: 27 August 2025

http://www.aimspress.com/journal/Math

Research article

Control protocol design for group consensus in heterogeneous multi-agent systems with communication interruptions and external disturbances

Yubin Zhong[1,2], Romana Ashfaq[3], Asad Khan[4,*], Azmat Ullah Khan Niazi[3,*], Taoufik Saidani[5], Adnan Burhan Rajab[6,7] and Mohammed M. A. Almazah[8]

[1] School of Mathematics and Information Science, Guangzhou University, Guangzhou 510006, China

[2] School of General Education, Guangzhou Institute of Science and Technology, Guangzhou 510540, China

[3] Department of Mathematics and Statistics, University of Lahore, Sargodha 40100, Pakistan

[4] Metaverse Research Institute, School of Computer Science and Cyber Engineering, Guangzhou University, Guangzhou 510006, China

[5] Center for Scientific Research and Entrepreneurship, Northern Border University, 73213, Arar, Saudi Arabia

[6] Department of Computer Engineering, College of Engineering, Knowledge University, Erbil 44001, Iraq

[7] Department of Computer Engineering, Al-Kitab University, Altun Kupri, Iraq

[8] Department of Mathematics, College of Sciences and Arts (Muhyil), King Khalid University, Muhyil 61421, Saudi Arabia

* **Correspondence:** Email: azmatniazi35@gmail.com, asad@gzhu.edu.cn.

Abstract: This paper studied the group consensus problem in heterogeneous multi-agent systems (HMASs) subject to input delays, denial of service (DoS) attacks, and external disturbances. The agents interact within a cooperative-competitive network, where first- and second-order dynamics coexist. To address the challenges introduced by disruptions in communication and system heterogeneity, an intermittent control protocol was designed. This protocol operates based on a time-varying binary signal that reflects the availability of communication. Control actions are suspended during DoS intervals and resume when communication is restored. The proposed method incorporates virtual velocity estimation to handle mixed-order agents and employs frequency-domain analysis, specifically the Nyquist stability criterion, to derive algebraic conditions that ensure consensus. These conditions relate the maximum allowable delay to system topology, attack patterns, and disturbance levels. Numerical simulations demonstrate that consensus can be achieved under both

directed and undirected network structures, even in the presence of constrained DoS disruptions and bounded disturbances.

Keywords: resilient group consensus; denial of service attacks; heterogeneous multi-agent systems; communication time delays; directed and undirected weighted graphs
Mathematics Subject Classification: 26A33, 34K37

1. Introduction

Multi-agent systems (MASs) are widely used to describe the coordinated behavior of interacting agents in distributed environments. Building on this, heterogeneous multi-agent systems (HMASs) incorporate agents with diverse dynamics and roles, better reflecting practical and complex scenarios such as advanced transportation systems, competition scenarios [1], and cyber-physical environments, owing to their capacity to manage agents with diverse dynamics and distributed control goals. These systems often function within networks that are subject to changes over time, requiring cooperative action among agents or reaching consensus despite challenges such as communication delays , external disturbances, and topology fluctuations. In particular, cooperative-competitive scenarios [2] where agents interact with both coordination-competition interplay, further complicate the design of reliable and stable control protocols. Input-related challenges, such as time delays and disturbances, have drawn increasing attention in the study of multi-agent systems. For instance, regulability and consensus behaviors under input delay have been examined in both nonlinear quaternion-valued systems and heterogeneous agent networks, while recent advances have addressed control input disruption induced by integrated disturbances-compensation strategies based on preview repetitive control [3].

Additionally, [4] demonstrated a paradoxical benefit in time-delayed coordination by demonstrating that intentional delays can enhance consensus achievement in second-order multi-agent systems.

In order to improve dynamic response control systems and the efficiency of communication transmission, event-triggered control strategies have attracted a lot of interest. In recent research, dynamic event-triggered leader-following consensus protocols that efficiently manage external disturbances in multi-agent systems and adaptive memory-based event-triggered strategies for finite-time lane-keeping in autonomous vehicles [5] have been investigated. Ensuring both fairness and transmission efficiency in UAV ad hoc networks presents a growing challenge, especially in multi-user multiple-input multiple-output (MIMO) settings. Recent research addresses this by jointly optimizing carrier sense multiple access with collision avoidance (CSMA/CA) protocols to balance performance and user access in such dynamic environments [6]. Consensus problems in multi-agent systems continue to draw extensive attention, particularly under challenging network conditions such as time delays and dynamic topologies. Recent research has shown that data-driven control with prioritized experience replay [7] and consensus under structural uncertainty has been addressed using the most exigent eigenvalue approach and extended to networks with both fixed and switching topologies.

Environment perception and adaptation have become critical in intelligent systems design. For instance, spatial memory-augmented reinforcement learning has been utilized to support visual navigation in unknown environments, while radar optimization techniques have been developed to

improve performance in spectrally crowded vehicular communication scenarios [8, 9]. In addition to perception and navigation under uncertain environments, recent studies have also focused on intelligent coordination and decision-making in multi-agent systems. Hypergraph-based models have been introduced to capture complex agent interactions in public decision-making scenarios, while zero-trust computing frameworks and deep reinforcement learning methods have been applied to enhance privacy security and task reliability in highly dynamic or extreme environments [10–12]. In the context of intelligent transportation systems, recent developments have focused on enhancing decision-making, trajectory planning, and perception under uncertain or constrained environments. A twisted Gaussian risk model was proposed [13] that accounts for the longitudinal-lateral motion states of surrounding vehicles to generate safer host vehicle trajectories.

To further improve control performance, an integrated decision-making and motion-planning framework has been developed [14] aimed at reducing oscillatory responses in dynamic driving conditions.

A control approach for robotic manipulators has been developed to achieve prescribed performance while handling system uncertainties through fuzzy-based adaptive robust techniques, as reported in [15]. Phase modulation plays a critical role in enhancing signal processing accuracy, especially under limited phase-shift conditions. Recent work has examined how periodic phase modulation impacts matched filtering performance in such constrained scenarios [16]. Recent work has also focused on improving tracking accuracy and system resilience in uncertain or adversarial environments. An automatic tracking system [17] for a microwave deicing device in railway contact lines, addressing control under operational constraints, was designed. To enhance path-following performance, a contour tracking approach was proposed [18] based on a time-varying internal model principle.

Robust signal acquisition and positioning under noisy conditions are essential for the reliability of modern intelligent systems. [19] proposed a fast Global Navigation Satellite System (GNSS) acquisition algorithm using sparse frequency transforms to improve localization under high-noise environments. [20] addressed high-frequency communication challenges by designing a low-noise amplifier. Meanwhile, [21] introduced ratio-based Visible Light Positioning (VLP), a technique for ambient light noise suppression in visible light positioning systems, enhancing accuracy in indoor localization. A distributed control scheme enables safe and coordinated platoon formation of connected and autonomous vehicles (CAVs) by addressing road curvature, merging, and actuation constraints [22].

Recent studies have proposed advanced control strategies to address nonlinearity, system constraints, cyber threats, and communication delays. Approaches such as adaptive pseudo inverse control, prescribed-performance design, and predefined-time output-feedback have been applied to robotic and aerospace systems [23–25]. Navigation-based methods and constraint-following control support motion planning in structured environments [26, 27], while resilient protocols incorporating deception-aware tracking and repetitive control enhance disturbance rejection [28, 29]. Additionally, Reinforcement learning and observer-based methods have been applied to achieve bipartite consensus and containment in heterogeneous and fractional-order multi-agent systems under delays [30]. In disaster-affected regions, maintaining reliable communication is essential for effective response and coordination. Recent studies have proposed multi-layer dissemination models with interference-aware strategies to enhance information flow under such challenging conditions [31].

Key advancements have addressed estimation security, system stability, and sensing coverage. security code estimation and replay (SCER) attacks have been studied by evaluating the tradeoff between code error and terminal gain [32]. Excessive emphasis on one can degrade the effectiveness of the other, making it vital to maintain an optimal balance. With the widespread use of digital processors in control systems, sampled-data control techniques have become fundamental for designing controllers that interact with continuous-time plants via discrete-time signals. Sampled-data control methods for Lurie systems and delay-dependent Lyapunov techniques have improved stability analysis [33, 34], which is used to maintain system stability and reliable performance, even when control actions are applied at discrete time intervals rather than continuously.

Sensor networks comprise spatially distributed nodes that collect and relay environmental or system data. These networks are integral to modern applications such as smart infrastructure, surveillance, and environmental monitoring. For sensor networks in irregular regions, k-coverage estimation enhances spatial reliability [35]. Minimizing energy consumption is a key challenge in wireless data collection from IoT sensors. Recent work explores session-specific optimization using deep reinforcement learning to improve efficiency in wirelessly powered networks [36].

Recent studies have also addressed distinct challenges in multi-agent coordination under complex constraints. For example, containment control with state constraints ensures that agents reach target regions while respecting physical or safety limits, making it essential in real-world multi-agent applications. Control with state constraints has been explored using event-triggered input strategies to enhance control performance in nonlinear systems [37]. Regret minimization in large agent populations has been modeled using a master equation framework, providing insight into adaptive decision-making in strategic environments [38]. This approach captures how agents adjust their strategies over time, offering a foundation for analyzing learning dynamics and equilibrium behavior in multi-agent systems. Furthermore, synchronization in quaternion-valued neural networks under neutral and discrete delays has been studied through aperiodic intermittent control, aiming to ensure stability in high-dimensional dynamic systems [39].

Moreover, delay-resilient protocols have been developed to maintain system performance and stability despite the presence of communication or input delays, which are common in networked and distributed control systems, including the improved proportional-integral-retarded (PIR) design for second-order MASs [40] and advanced delay-domain techniques such as Cluster treatment of characteristic roots (CTCR) and Dixon resultant theory have been employed to characterize stability under distributed delays, offering a precise framework for analyzing robustness in time-delay multi-agent systems [41]. Nevertheless, these approaches typically overlook the challenges posed by mixed-order agent configurations and the simultaneous presence of communication interruptions and external disturbances.

In certain control scenarios, integrating human judgment into the decision-making loop enhances system flexibility and safety, particularly in applications such as autonomous driving, remote surgery, and industrial automation, where fully autonomous strategies may fall short under uncertainty or dynamic conditions. Recently, efforts have turned to integrating human-in-the-loop (HiTL) feedback and event-triggered communication (ETC) schemes into MAS coordination. One study proposed a fully distributed formation control strategy under asynchronous edge-triggered communication, leveraging output transformation and observer design to handle unknown actuator and sensor disturbances [42]. Another line of research tackled output consensus for nonlinear systems under

sensor uncertainty and disturbance, using interval observers to reconstruct unknown dynamics and support distributed controller design [43].

Considerable progress has been reported in the above studies on networked systems; however, many of these works tend to address individual issues such as communication delays, external disturbances, or changes in network topology in isolation. While these contributions form a strong foundation and are acknowledged in this work, there is still a clear need for unified approaches that can handle multiple practical constraints at once, especially under complex and dynamic conditions. In particular, the combined impact of cyber attacks, such as denial-of-service (DoS), and agent heterogeneity in dynamic network settings remains insufficiently explored. To address this gap, this paper proposes an integrated control framework that ensures robust consensus performance under communication interruptions, dynamic agent behavior, and adversarial disruptions. The main contributions of this work are outlined below.

Main Contributions: The key contributions of this paper are summarized as follows:

- A novel group consensus protocol is proposed for heterogeneous multi-agent systems (HMASs) consisting of both first- and second-order agents operating under cooperative-competitive interactions.
- The control strategy explicitly incorporates input delays, denial of service (DoS) attacks, and external disturbances, enhancing robustness in adverse communication environments.
- A virtual velocity framework is introduced to standardize the dynamics of first-order agents, enabling unified consensus control alongside second-order agents within the same coordination protocol.
- Frequency-domain analysis is conducted to derive algebraic conditions for consensus stability, providing delay bounds in terms of system topology, disturbance levels, and DoS activity.
- Extensive simulations under both directed and undirected communication topologies validate the theoretical findings and demonstrate the practical viability of the proposed approach.

The rest of the document is structured as follows:

(1) In Section 2, the topic is described, including an introduction to the basics of graph theory.

(2) Section 3 presents the principal results concerning group consensus (GC) for heterogeneous multi-agent systems (HMASs) with input delays.

(3) Section 4 describes a number of simulations.

(4) In the conclusion, Section 5, we provide an overview of the research results and recommendations for further investigation.

Notation: Consider a directed weighted graph $\mathcal{G} = (\mathcal{V}, \mathcal{E})$, where the nodes are represented by $\mathcal{V} = \{v_1, v_2, \ldots, v_n\}$ and indexed by the set $\mathcal{N} = \{1, 2, \ldots, n\}$. The edges between nodes are given by $\mathcal{E} \subseteq \mathcal{V} \times \mathcal{V}$. The adjacency matrix $\mathcal{B} = [a_{ij}] \in \mathbb{R}^{n\times n}$ is defined such that $a_{ij} \neq 0$ if $(v_i, v_j) \in \mathcal{E}$; otherwise, $a_{ij} = 0$. An edge $e_{ij} = (v_i, v_j) \in \mathcal{E}$ indicates a directed link from v_j to v_i. Positive (negative) values of a_{ij} signify cooperative (antagonistic) interactions between nodes v_i and v_j. It is assumed that $a_{ii} = 0$ for each $i \in \mathcal{N}$. For any node i , its neighboring nodes are represented as $\mathcal{N}_i = \{j \in \mathcal{V} : e_{ij} \in \mathcal{E}\}$. The Laplacian matrix $\mathcal{L}$ of graph $\mathcal{G}$ is defined by $\mathcal{L} = \mathcal{D} - \mathcal{A}$, where $\mathcal{D} = \text{diag}\{d_1, d_2, \ldots, d_n\}$ with $d_i = \sum_{j\neq i} |a_{ij}|$. Matrix $\mathcal{L}$ satisfies $\mathcal{L}\mathbf{1}_n = \mathbf{0}_n$, where $\mathbf{1}_n$ and $\mathbf{0}_n$ are $n\times 1$ vectors with all elements equal to 1

and 0, respectively. We define the following notations: $\mathbb{R}$ denotes the set of real numbers, and $\mathbb{C}$ denotes the set of complex numbers. For any $z \in \mathbb{C}$, $\mathcal{R}(z)$ and $\mathcal{I}(z)$ represent its real and imaginary components, respectively. Additionally, $\mathbb{R}^{m\times n}$ is the set of $m \times n$ real matrices, $\mathcal{I}_n$ represents the identity matrix of order n, $\lambda_i(\cdot)$ denotes the i-th eigenvalue of a matrix, and $\det(\cdot)$ is used for the matrix determinant.

In this context, denial of service (DoS) attacks are symbolized by η, and external disturbances are represented by ζ, both of which are included in our system analysis.

2. Problem formulation

In this study, we explore a mixed-order multi-agent system (MAS) comprising m second-order agents and n first-order agents, aiming to understand their dynamics in the face of communication disruptions caused by denial of service (DoS) attacks. The second-order agents, denoted as $Q_1 = \{1, 2, \ldots, m\}$, are governed by the following dynamic equations:

$$\dot{\xi}_i(t) = \psi_i(t), \quad \dot{\psi}_i(t) = u_i(t) + \zeta_i(t), \quad i \in Q_1, \tag{2.1}$$

where $\xi_i(t)$, $\psi_i(t)$ and $u_i(t)$ represent the position, velocity, and control input of the i-th second-order agent, respectively, and $\zeta_i(t)$ denotes the uncertain external disturbances. For simplicity, we focus on the one-dimensional case ($r = 1$), meaning

$$\xi_i(t), \psi_i(t), u_i(t) \in \mathbb{R}.$$

Analogous results hold for $r > 1$.

The rest of the n agents, labeled as $Q_2 = \{m + 1, m + 2, \ldots, m + n\}$, follow first-order dynamics described by:

$$\dot{\xi}_i(t) = u_i(t) + \zeta_i(t), \quad i \in Q_2, \tag{2.2}$$

where $\xi_j(t)$ and $u_j(t)$ represent the position and control input of the j-th first-order agent, respectively.

The agents are grouped into s subgroups, where each agent i belongs to a subgroup j, represented as $\Delta_i = j$. Our main focus is on the scenario with $s = 2$, though the results can extend to cases with more subgroups.

Definition 2.1. (Group Consensus (GC))

The MAS asymptotically reaches group consensus if, for any beginning conditions, the agent states meet the following criteria:

For agents within the same subgroup:

$$\lim_{t\to\infty} \|\xi_i(t) - \xi_j(t)\| = 0, \quad \lim_{t\to\infty} \|\psi_i(t) - \psi_j(t)\| = 0, \quad \text{if } \Delta_i = \Delta_j.$$

For agents in different subgroups:

$$\lim_{t\to\infty} \|\xi_i(t) - \xi_j(t)\| \neq 0, \quad \lim_{t\to\infty} \|\psi_i(t) - \psi_j(t)\| \neq 0, \quad \text{if } \Delta_i \neq \Delta_j.$$

Let $i, j \in \{1, 2, \ldots, N\}$ be the indices of agents, where N is the total number of agents, and $\Delta_i, \Delta_j \in \{1, 2, \ldots, M\}$ indicate the subgroup to which each agent belongs. The adjacency matrix A can be expressed in the following form, which corresponds to the partitioning of different subgroups.

$$A = \begin{bmatrix} A_{11} & A_{12} \\ A_{21} & A_{22} \end{bmatrix}.$$

Here, A_{11} indicates the inter-agent communication within subgroup 1, capturing interactions that occur exclusively among its members. Similarly, A_{22} describes the intra-group information exchange specific to subgroup 2. On the other hand, A_{12} and A_{21} represent inter-subgroup interactions, reflecting the communication between agents belonging to subgroups 1 and 2. To formalize the concept, we now present the following definition.

$$B = \begin{bmatrix} -A_{11} & A_{12} \\ A_{21} & -A_{22} \end{bmatrix}.$$

Agents within the same subgroup interact cooperatively, aiming to maintain consistent relative positions. In contrast, agents from different subgroups exhibit competitive dynamics, which involve sustaining opposite positioning between them. To capture this cooperative-competitive structure in the context of HMASs, the adjacency matrix B is constructed by assigning opposite values to A_{11} and A_{22}, effectively representing the nature of interactions both within and across subgroups

Note: A negative weight (-1) in the adjacency matrix $\mathcal{B}$ induces strictly competitive interactions where connected agents actively oppose each other's state evolution, creating divergent dynamics that drive system polarization. This antagonistic coupling manifests in the block matrix structure $\mathcal{B}$, where the negated diagonal elements $(-\mathcal{A}_{11}, -\mathcal{A}_{22})$ enforce intra-subgroup competition while the off-diagonal blocks $(\mathcal{A}_{12}, \mathcal{A}_{21})$ govern inter-subgroup interactions. Through the Laplacian transformation $\mathcal{L} = \mathcal{D} - \mathcal{B}$, these intra-group competitive terms become effective cooperative couplings, enabling local consensus within subgroups while preserving global divergence between them. The resulting dynamics-where local convergence and global separation coexist-find application in polarized opinion formation, adversarial swarm control, and biological systems with competing subgroups, demonstrating how strategically opposed interactions can produce stable emergent patterns in heterogeneous multi-agent networks.

Remark 2.1. *Many existing system models focus on homogeneous agents and treat either cooperative or competitive [1] interactions separately. In contrast, the proposed framework considers a heterogeneous multi-agent system (HMAS) that includes both first- and second-order agents. It simultaneously captures cooperative and competitive dynamics [2] and also addresses realistic factors such as input delays, DoS attacks, and external disturbances. This unified approach offers a more practical and generalizable model compared to conventional designs.*

Definition 2.2. (Communication Disruption Attacks)

In cyber-physical systems (CPSs), communication disruption attacks (denoted as $\{C_\alpha\}_{\alpha=1}^{\infty}$) pose significant threats by disrupting the communication channels required for coordination. Each disruption starts at time C_α and lasts for a duration Δ_α, adhering to the condition:

$$C_{\alpha+1} > C_\alpha + \Delta_\alpha.$$

During a disruption, agents are unable to communicate. The duration of communication failure in the interval $[t_0, t]$ is expressed as:

$$\Lambda_f = \bigcup_{\alpha} [C_\alpha + \Delta_\alpha] \cap [t_0, t].$$

The available communication time in the interval $[t_0, t]$ is:

$$\Lambda_c = [t_0, t] \setminus \Lambda_f.$$

Definition 2.3. (Disruption Frequency and Disruption Length Ratio)

The disruption frequency $F(t_0, t)$ over the interval $[t_0, t]$ is defined as:

$$F(t_0, t) = \frac{n_\gamma(t_0, t)}{t - t_0},$$

where $n_\gamma(t_0, t)$ is the total number of disruptions during this interval.

The disruption length ratio ρ_d is defined as the ratio of communication failure time to the total time:

$$\rho_d = \frac{\Lambda_f(t_0, t)}{t - t_0}.$$

Redundancy removal in a communication graph

Consider the communication graph G_T defined as:

$$A|_T = [a_{ij}] = \begin{cases} 0, & (i, j) \notin E|_T, \\ a_{ij}, & (i, j) \in E|_T. \end{cases}$$

This graph represents the active edges after redundancy removal, ensuring that only essential communication links remain under communication disruption attacks.

Lemma 2.2. *Under the influence of a denial of Service (DoS) attack, the inequality* $\frac{\theta}{1+\theta^2} < \arctan(\theta)$ *holds for* $\theta > 0$ *exclusively during communication intervals, defined as* $\Lambda_c = [t_0, t] \setminus \Lambda_f$*, where* $\Lambda_f = \bigcup_\alpha [C_\alpha + \Delta_\alpha] \cap [t_0, t]$ *represents the set of times affected by the DoS attack.*

Proof. Let us define the function

$$\gamma(\theta) = \frac{\theta}{1 + \theta^2} - \arctan(\theta).$$

The derivative of this function is given by

$$\gamma'(\theta) = -\frac{2\theta^2}{(1 + \theta^2)^2}.$$

Since $\theta > 0$, it follows that $\gamma'(\theta) < 0$, indicating that $\gamma(\theta)$ is monotonically decreasing. Evaluating the function at zero, we find

$$\gamma(0) = 0,$$

which implies that for $\theta > 0$,

$$\gamma(\theta) < 0.$$

This result demonstrates that the inequality holds during the intervals when communication is operational, specifically during Λ_c, where agents are free from the disruptions caused by DoS attacks. Hence, the validity of the inequality is contingent on maintaining effective communication channels. □

3. Main results

In real-world multi-agent systems (MASs), agents engage in both cooperative and competitive interactions. These interactions are represented as a sum for $\xi_i + \xi_j$ competitive behavior, and as a difference $\xi_i - \xi_j$ for cooperative behavior. Let N_{i1} represent the neighboring agents in the same subgroup as agent i, and N_{i2} denote agents from different subgroups.

Achieving a consensus in cooperative-competitive interactions in heterogeneous systems with multiple agents, we propose a control protocol that manages agent interactions to ensure consensus, even in the presence of delays and network disruptions. In response to denial of service (DoS) attacks, the protocol incorporates a time-varying indicator function $\eta(t)$ that monitors communication between agents. The function $\eta(t)$ takes values in $\{0, 1\}$:

$$\eta(t) = 1 : \text{Communication is active (no DoS attack)},$$

$$\eta(t) = 0 : \text{Communication is disrupted due to a DoS attack.}$$

This function models DoS attacks by permitting interactions only when $\eta(t) = 1$.

Control Protocol under DoS Attacks:

For agents $i \in Q_1$, the dynamics under DoS attacks are modified as follows:

$$\dot{\xi}_i(t) = \psi_i(t), \tag{3.1a}$$

$$\begin{aligned}\dot{\psi}_i(t) = &-\kappa\left(\eta(t)\sum_{j\in N_{i1}} b_{ij}(\xi_i(t) - \xi_j(t)) + \eta(t)\sum_{j\in N_{i2}} b_{ij}(\xi_i(t) + \xi_j(t))\right)\\ &-\gamma\left(\eta(t)\sum_{j\in N_{i1}} b_{ij}(\psi_i(t) - \psi_j(t)) + \eta(t)\sum_{j\in N_{i2}} b_{ij}(\psi_i(t) + \psi_j(t))\right) + \zeta_i(t),\end{aligned} \tag{3.1b}$$

where $\eta(t)$ determines the communication status at time t and $\zeta_i(t)$ represent the external disturbance affecting the agent.

For agents $i \in Q_2$, the dynamics are given by:

$$\dot{\xi}_i(t) = -\gamma\left(\eta(t)\sum_{j\in N_{i1}} b_{ij}(\xi_i(t) - \xi_j(t)) + \eta(t)\sum_{j\in N_{i2}} b_{ij}(\xi_i(t) + \xi_j(t))\right) + \omega_i(t) + \zeta_i(t), \tag{3.2a}$$

$$\dot{\omega}_i(t) = -\kappa\left(\eta(t)\sum_{j\in N_{i1}} b_{ij}(\xi_i(t) - \xi_j(t)) + \eta(t)\sum_{j\in N_{i2}} b_{ij}(\xi_i(t) + \xi_j(t))\right), \tag{3.2b}$$

where $\omega_i(t)$ represents the velocity estimate of agent $i \in Q_2$, $\eta(t)$ modulates the communication effects, and $\zeta_i(t)$ again accounts for external disturbance.

Consensus Protocol with Input Delays under DoS Attacks:

Now, consider the system's behavior with input delay τ and DoS attacks. The dynamics for agents $i \in Q_1$ are:

$$\dot{\xi}_i(t) = \psi_i(t), \tag{3.3a}$$

$$\dot{\psi}_i(t) = -\kappa\left(\eta(t)\sum_{j\in N_{i1}} b_{ij}(\xi_i(t-\tau)-\xi_j(t-\tau)) + \eta(t)\sum_{j\in N_{i2}} b_{ij}(\xi_i(t-\tau)+\xi_j(t-\tau))\right)$$
$$-\gamma\left(\eta(t)\sum_{j\in N_{i1}} b_{ij}(\psi_i(t-\tau)-\psi_j(t-\tau)) + \eta(t)\sum_{j\in N_{i2}} b_{ij}(\psi_i(t-\tau)+\psi_j(t-\tau))\right) + \zeta_i(t), \tag{3.3b}$$

where $\eta(t)$ models the time-dependent communication disruptions due to DoS attacks.

For agents $i \in Q_2$, the dynamics are:

$$\dot{\xi}_i(t) = -\gamma\left(\eta(t)\sum_{j\in N_{i1}} b_{ij}(\xi_i(t-\tau)-\xi_j(t-\tau)) + \eta(t)\sum_{j\in N_{i2}} b_{ij}(\xi_i(t-\tau)+\xi_j(t-\tau))\right) + \omega_i(t) + \zeta_i(t), \tag{3.4a}$$

$$\dot{\omega}_i(t) = -\kappa\left(\eta(t)\sum_{j\in N_{i1}} b_{ij}(\xi_i(t-\tau)-\xi_j(t-\tau)) + \eta(t)\sum_{j\in N_{i2}} b_{ij}(\xi_i(t-\tau)+\xi_j(t-\tau))\right). \tag{3.4b}$$

Theorem 3.1. *For the heterogeneous multi-agent systems (HMASs) represented by Eqs (3.3) and (3.4), asymptotic group consensus (GC) can be achieved under these terms:*

(i) $rank(\mathcal{D}+\mathcal{B}) = m+n-1$;
(ii) *Every nonzero eigenvalue is positive;*
(iii) $\frac{\left(\lambda_i\sqrt{\kappa^2+\gamma^2\omega_{i0}^2}\right)\eta(jw)+|\zeta_i(j\omega)|}{\omega_{i0}^2} < 1$;

where λ_i *is the i-th nonzero eigenvalue of matrix* $D+B$, $\eta(j\omega)$ *represents the DoS attack,* $\zeta(j\omega)$ *is the external disturbance, and* ω_{i0} *satisfies* $\tan(\omega_{i0}\tau) = \frac{\gamma\omega_{i0}}{\kappa}$.

Proof. Taking the Laplace transform on both sides of Eqs (3.3) and (3.4), we obtain, for any agent $i \in Q_1$,

$$s\Xi_i(s) = \Psi_i(s), \tag{3.5a}$$

$$s\Psi_i(s) = -\kappa\left(\eta(s)\sum_{j\in\mathcal{N}_i^1} b_{ij}(\Xi_i(s)-\Xi_j(s))e^{-s\tau} + \eta(s)\sum_{j\in\mathcal{N}_i^2} b_{ij}(\Xi_i(s)+\Xi_j(s))e^{-s\tau}\right)$$
$$-\gamma\left(\eta(s)\sum_{j\in\mathcal{N}_i^1} b_{ij}(\Psi_i(s)-\Psi_j(s))e^{-s\tau} + \eta(s)\sum_{j\in\mathcal{N}_i^2} b_{ij}(\Psi_i(s)+\Psi_j(s))e^{-s\tau}\right) + \zeta_i(s), \tag{3.5b}$$

and for any of the agents $i \in Q_2$,

$$s\Xi_i(s) = -\gamma\left(\eta(s)\sum_{j\in\mathcal{N}_i^1} b_{ij}(\Xi_i(s)-\Xi_j(s))e^{-s\tau} + \eta(s)\sum_{j\in\mathcal{N}_i^2} b_{ij}(\Xi_i(s)+\Xi_j(s))e^{-s\tau}\right) + \Omega_i(s) + \zeta_i(s), \tag{3.6a}$$

$$s\Omega_i(s) = -\kappa\left(\eta(s)\sum_{j\in\mathcal{N}_i^1} b_{ij}(\Xi_i(s)-\Xi_j(s))e^{-s\tau} + \eta(s)\sum_{j\in\mathcal{N}_i^2} b_{ij}(\Xi_i(s)+\Xi_j(s))e^{-s\tau}\right), \tag{3.6b}$$

where the Laplace transforms of $\xi_i(t)$, $\psi_i(t)$, $\eta(t)$, $\zeta_i(t)$, and $\omega_i(t)$ are denoted by $\Xi_i(s)$, $\Psi_i(s)$, $\eta(s)$, $\zeta_i(s)$, and $\Omega_i(s)$, respectively. Let $\Xi(s) = [\Xi_1(s), \Xi_2(s), \ldots, \Xi_{m+n}(s)]^T$. Then, according to Eqs (3.5) and (3.6), the following result can be obtained:

$$s^2\Xi(s) = -(\kappa + \gamma s)e^{-s\tau}\eta(s)(\mathcal{D} + \mathcal{B})\Xi(s) + \zeta_i(s). \tag{3.7}$$

Furthermore, the characteristic equation for Eqs (3.5) and (3.6) can be formulated as:

$$\det\left(s^2 I + (\kappa + \gamma s)e^{-s\tau}\eta(s)(\mathcal{D} + \mathcal{B}) + \zeta_i(s)I\right) = 0. \tag{3.8}$$

Define $\varphi(s) = \det\left(s^2 I + (\kappa + \gamma s)e^{-s\tau}\eta(s)(\mathcal{D} + \mathcal{B}) + \zeta_i(s)I\right)$; it follows that $\varphi(0) = \det(0)$. Given condition (i) that $\text{rank}(\mathcal{D} + \mathcal{B}) = m + n - 1$, we deduce that $(\mathcal{D} + \mathcal{B})$ has rank $m + n - 1$, indicating that zero is an eigenvalue of $\mathcal{D} + \mathcal{B}$ with all other eigenvalues being positive real numbers. Consequently, $\varphi(s)$ has a zero at $s = 0$. For $s \neq 0$, based on Eq (3.8), we have

$$1 + \frac{\lambda_i\eta(s)(\kappa + \gamma s)}{s^2}e^{-s\tau} + \frac{\zeta_i(s)}{s^2} = 0, \quad i = 2, \ldots, m + n. \tag{3.9}$$

Equation (3.9) can be rewritten as $1 + \varphi_i(s) = 0$, where $\varphi_i(s)$ is defined as $\frac{\lambda_i(\kappa+\gamma s)e^{-s\tau}}{s^2} + \frac{\zeta_i(s)}{s^2}$. Utilizing the criterion of Nyquist stability, we just need to examine the characteristics of $\varphi_i(s)$. The left-half complex plane contains the roots of Eq (3.9) if and only if the point $(-1, j0)$ is not surrounded by the Nyquist curve $\varphi_i(j\omega)$ for any $\omega \in \mathbb{R}$. By setting $s = j\omega$ for $\omega \in \mathbb{R}$ and engaging in some manipulation, we obtain

$$\varphi_i(j\omega) = \frac{\lambda_i}{-\omega^2}\left((\kappa\cos\omega\tau + \gamma\omega\sin\omega\tau) + j(\gamma\omega\cos\omega\tau - \kappa\sin\omega\tau)\right)\eta(s) + \frac{\zeta_i(s)}{\omega^2}, \tag{3.10}$$

$$|\varphi_i(j\omega)| = \frac{\left(\lambda_i\sqrt{\kappa^2 + \gamma^2\omega^2}\right)\eta(jw) + |\zeta_i(j\omega)|}{\omega^2}, \tag{3.11}$$

and

$$\arg(\varphi_i(j\omega)) = -\omega\tau + \arctan\left(\frac{\gamma\omega}{\kappa}\right)\eta(jw) - \pi + \arg(\zeta_i(jw)). \tag{3.12}$$

From Eq (3.11), $|\varphi_i(j\omega)|$ decreases monotonically since $\omega > 0$. Considering that the curve $\varphi_i(j\omega)$ first intersects the real axis at ω_{i0}, we find $\arg(\varphi_i(j\omega)) = -\pi$, which implies $\tan(\omega_{i0}\tau) = \frac{\gamma\omega_{i0}}{\kappa}$. Consequently, it is both required and adequate for the zeros of $1 + \varphi_i(s)$ in Eq (3.9) to have actual negative components when $|\varphi_i(j\omega)| = \frac{\left(\lambda_i\sqrt{\kappa^2+\gamma^2\omega_{i0}^2}\right)\eta(jw)+|\zeta_i(j\omega)|}{\omega_{i0}^2} < 1$. Thus, achieving group consensus for the HMASs requires that both hypothetical conditions $\frac{\left(\lambda_i\sqrt{\kappa^2+\gamma^2\omega_{i0}^2}\right)\eta(jw)+|\zeta_i(j\omega)|}{\omega_{i0}^2} < 1$ and $\tan(\omega_{i0}\tau) = \frac{\gamma\omega_{i0}}{\kappa}$ hold. □

Assumption 3.1. Denial of service (DoS) assaults, as described in condition (iii), have a restricted impact and are bounded in their influence within the Nyquist stability criterion. As in condition (iii), the external disturbance denoted by $\zeta_i(s)$ is also bounded and does not exceed the specified threshold, guaranteeing that its impact on system stability is kept under control. All of these ensure that external disruptions and DoS attacks are adequately managed, allowing the system to remain stable and reach consensus.

Remark 3.2. *The proposed framework handles denial of service (DoS) attacks and external disturbances through distinct mechanisms. A binary function $\eta(t) \in \{0, 1\}$ represents the communication status, where $\eta(t) = 1$ indicates active communication and $\eta(t) = 0$ represents a DoS interval. During inactive periods, control inputs are suspended, resulting in an intermittent control protocol that maintains system stability despite communication loss. External disturbances are modeled as bounded unknown inputs, and the control protocol ensures robustness by keeping consensus errors bounded. These two effects are jointly addressed in the stability conditions derived using the Nyquist stability criterion.*

Remark 3.3. *To keep their impact under control, condition (iii) establishes a critical threshold for the combined consequences of external disruptions and denial of service (DoS) attacks. This condition minimizes the influence of $\eta(j\omega)$ and $\zeta_i(j\omega)$ so that $|\varphi_i(j\omega)| < 1$ at frequency ω_{i0}, preventing disruptive forces from overpowering the system and preserving the stability necessary for group consensus. Even in the face of adversity, this threshold serves as a safety net, enabling agents to align their states and reach consensus.*

Theorem 3.4. *The following condition must be met for HMASs (3.3) and (3.4) to asymptotically reach consensus by Theorem 3.1:*

$$\tau < \min\left(\frac{\arctan\left(\frac{\gamma}{\kappa}\vartheta\right)\eta(j\omega) + \arg(\zeta_i(j\omega))}{\vartheta}\right), \tag{3.13}$$

where $\vartheta = \sqrt{\left(\lambda_i\sqrt{\kappa^2+\gamma^2\omega_{i0}^2}\right)\eta(j\omega) + |\zeta_i(j\omega)|}$ and $\eta(j\omega)$, $\zeta(j\omega)$, λ_i signify the DOS attacks on the communication, external disturbance affecting the system, and nonzero eigenvalues with $i \in Q$, respectively.

Proof. With reference to Eq (3.12), one can obtain: $\arg(g_i(j\omega_{i0})) = -\omega_{i0}\tau + \arctan\left(\frac{\gamma\omega_{i0}}{\kappa}\right)\eta(j\omega) - \pi + arg(\zeta_i(j\omega)) = -\pi$, which yields

$$\tau = \frac{\arctan\left(\frac{\gamma}{\kappa}\omega_{i0}\right)\eta(j\omega) + \arg(\zeta_i(j\omega))}{\omega_{i0}}. \tag{3.14}$$

Equation (3.14) thus yields the rate of change of τ with regard to ω_{i0} :

$$\frac{d\tau}{d\omega_{i0}} = \frac{1}{\omega_{i0}^2}\left(\frac{\gamma\omega_{i0}/\kappa}{1+(\gamma\omega_{i0}/\kappa)^2} - \arctan\left(\frac{\gamma\omega_{i0}}{\kappa}\right) - \arg(\zeta_i(jw)\right). \tag{3.15}$$

A consequence of Lemma 2.2 shows that $\frac{d\tau}{d\omega_{i0}} < 0$ for $\omega_{i0} > 0$. In other words, the time delay τ gradually decreases as ω_{i0} increases.

Concurrently, the Nyquist stability criteria imply that the amplitude limit of $g_i(j\omega)$ necessitates the condition $\frac{\left(\lambda_i\sqrt{\kappa^2+\gamma^2\omega_{i0}^2}\right)\eta(jw)+|\zeta_i(j\omega)|}{\omega_{i0}^2} < 1$. As a result of mathematical manipulation, it is equivalent to

$$\omega_{i0} > \sqrt{\left(\lambda_i\sqrt{\kappa^2+\gamma^2\omega_{i0}^2}\right)\eta(jw) + |\zeta_i(j\omega)|}. \tag{3.16}$$

Therefore, we assess the following result regarding the upper bound of input delay by combining Eqs (3.14) and (3.16):

$$\tau < \left(\frac{\arctan\left(\frac{\gamma}{\kappa}\vartheta\right)\eta(j\omega) + \arg(\zeta_i(j\omega))}{\vartheta} \right). \tag{3.17}$$

□

Remark 3.5. *The nonzero eigenvalues inclusion in the study highlights how the structure of the system affects the stability margins. The topology and dynamics of the system are linked to its consensus behavior through the direct influence of the eigenvalues on the input delay bounds.*

Remark 3.6. *These findings underscore the importance of properly managing input delays and disturbances in the design and deployment of high-order multi-agent systems (HOMASs), highlighting the need for effective control mechanisms that account for the limitations outlined in Theorem 3.4 to ensure reliable performance and dependability in the face of potential disruptions.*

Remark 3.7. *The algebraic criteria proposed in Theorems 3.1 and 3.4 apply to heterogeneous multi-agent systems with fixed communication topologies, constant input delays, and bounded external disturbances. The effectiveness of these results depends on the rank condition* $rank(\mathcal{D} + \mathcal{B}) = m + n - 1$, *which ensures a connected network, and on the positivity of all nonzero eigenvalues of* $\mathcal{D} + \mathcal{B}$. *The bounds involving the DoS signal* $\eta(s)$ *and disturbance* $\zeta_i(s)$ *must be satisfied according to the frequency-domain stability condition outlined in Theorem 3.1.*

These conditions may not remain valid in cases involving switching topologies, time-varying delays, or unbounded disturbances. If the structural conditions on $\mathcal{D} + \mathcal{B}$ *are violated, such as the loss of connectivity or presence of zero nontrivial eigenvalues, the consensus behavior cannot be guaranteed. In such scenarios, alternative control approaches, possibly using adaptive or robust methods, may be required to maintain system stability.*

Remark 3.8. *The proposed control strategy is fully distributed, meaning each agent updates its control input using only local information from its neighbors without relying on centralized coordination or global knowledge. Each update step involves basic arithmetic operations on the agent's own state and the virtual velocity term, resulting in low per-agent computational cost. No matrix inversion, optimization, or global communication is required. As supported by the simulation results under both directed and undirected topologies, the method remains efficient and scalable even in the presence of adverse conditions, making it suitable for real-time applications in large-scale heterogeneous networks.*

4. Simulation results

The structure of the proposed model is illustrated in Figure 1. Based on this configuration, the following numerical simulations demonstrate that all agents achieve consensus under the proposed control strategy, despite the presence of input delays, external disturbances, and denial-of-service (DoS) attacks. The numerical simulations are presented as follows.

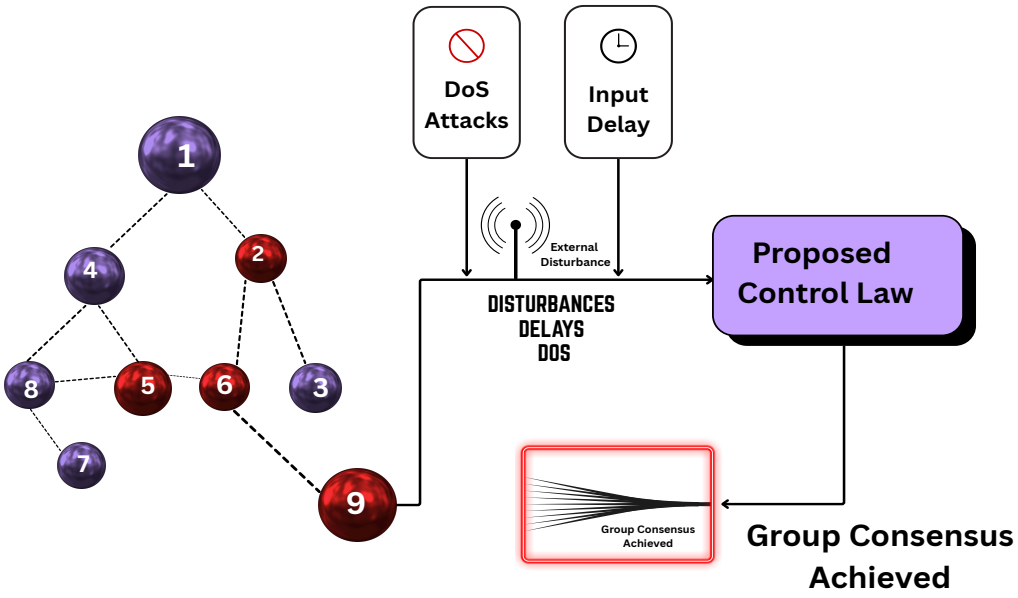

Figure 1. System evolution.

Example 4.1. (Directed Topology) In this example, we analyze a heterogeneous multi-agent system comprising nine agents, categorized into two subgroups.

The first subgroup includes agents 1–4, while the second subgroup consists of agents 5–9. Agents 2, 5, 6, and 9 belong to Q_1 and agents 1, 3, 4, 7, and 8 belong to Q_2, introducing heterogeneity in the system structure.

From Figure 2,

$$\mathcal{D} = \begin{bmatrix} 1 & 0 & 0 & 0 & 0 & 0 & 0 & 0 & 0 \\ 0 & 1 & 0 & 0 & 0 & 0 & 0 & 0 & 0 \\ 0 & 0 & 1 & 0 & 0 & 0 & 0 & 0 & 0 \\ 0 & 0 & 0 & 2 & 0 & 0 & 0 & 0 & 0 \\ 0 & 0 & 0 & 0 & 3 & 0 & 0 & 0 & 0 \\ 0 & 0 & 0 & 0 & 0 & 1 & 0 & 0 & 0 \\ 0 & 0 & 0 & 0 & 0 & 0 & 0 & 0 & 0 \\ 0 & 0 & 0 & 0 & 0 & 0 & 0 & 1 & 0 \\ 0 & 0 & 0 & 0 & 0 & 0 & 0 & 0 & 1 \end{bmatrix}$$

$$\mathcal{B} = \begin{bmatrix} 0 & 1 & 0 & 0 & 0 & 0 & 0 & 0 & 0 \\ 1 & 0 & 0 & 0 & 0 & 0 & 0 & 0 & 0 \\ 0 & -1 & 0 & 0 & 0 & 0 & 0 & 0 & 0 \\ 1 & 0 & 0 & 0 & 0 & 0 & 0 & 1 & 0 \\ 0 & 0 & 0 & -1 & 0 & 1 & 0 & 1 & 0 \\ 0 & 1 & 0 & 0 & 0 & 0 & 0 & 0 & 0 \\ 0 & 0 & 0 & 0 & 0 & 0 & 0 & 0 & 0 \\ 0 & 0 & 0 & 0 & 0 & 0 & -1 & 0 & 0 \\ 0 & 0 & 0 & 0 & 0 & 1 & 0 & 0 & 0 \end{bmatrix}$$

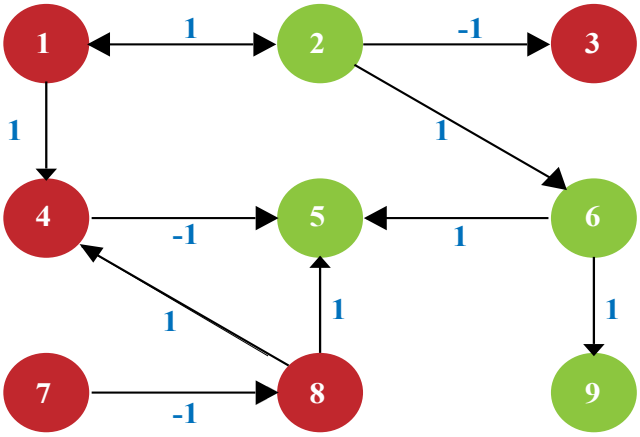

Figure 2. Directed topology of nine agents.

The combined matrix $\mathcal{D}+\mathcal{B}$, representing the overall communication topology, is as follows:

$$\mathcal{D}+\mathcal{B}=\begin{bmatrix}1&1&0&0&0&0&0&0&0\\1&1&0&0&0&0&0&0&0\\0&-1&1&0&0&0&0&0&0\\1&0&0&2&0&0&0&1&0\\0&0&0&-1&3&1&0&1&0\\0&1&0&0&0&1&0&0&0\\0&0&0&0&0&0&0&0&0\\0&0&0&0&0&0&-1&1&0\\0&0&0&0&0&1&0&0&1\end{bmatrix}$$

The eigenvalues of the combined matrix, $\mathcal{D}+\mathcal{B}$, are calculated as:

$$\lambda_1=1,\lambda_2=3,\lambda_3=2,\lambda_4=1,\lambda_5=1,\lambda_6=2,\lambda_7=0,\lambda_8=1,\lambda_9=0.$$

Assume $\kappa=20$ and $\gamma=10$. The initial positions of the nine agents are defined as follows: $\xi_1(0)=-8$, $\xi_2(0)=-4$, $\xi_3(0)=-2$, $\xi_4(0)=3$, $\xi_5(0)=7$, $\xi_6(0)=9$, $\xi_7(0)=1$, $\xi_8(0)=5$, $\xi_9(0)=2$. Additionally, all agents' initial velocities are set to zero uniformly. To further analyze this system, we consider the impact of denial of service (DoS) attacks and external disturbances. By performing simple calculations based on Theorems 3.1 and 3.4, we find that the input delay must be less than 0.35 seconds. This indicates that group consensus in heterogeneous multi-agent systems can be achieved under the directed topology as long as the input delay is below 0.35 seconds.

We evaluate the system for input delay values of 0.33 seconds, 0.35 seconds, and 0.37 seconds, with the correspondence state of position and velocity illustrated in Figures 3–5.

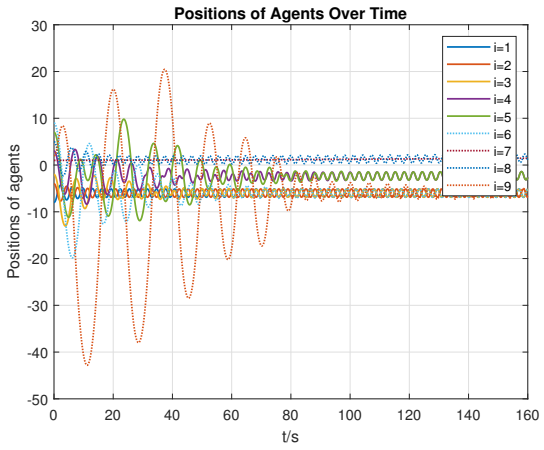

(a) Position

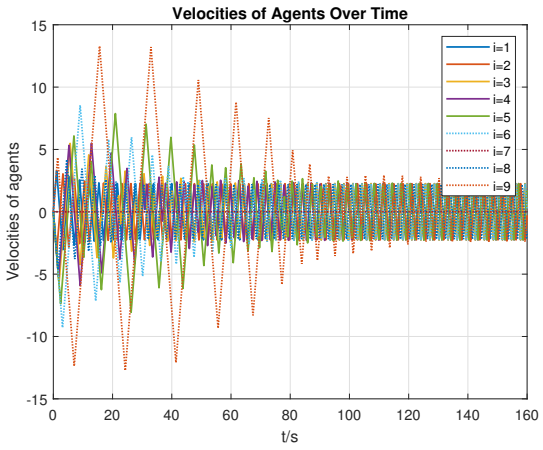

(b) Velocity

Figure 3. Heterogeneous multi-agent systems (HMASs) with a time delay of $\tau = 0.33$ s are analyzed under the topology configuration in Figure 2.

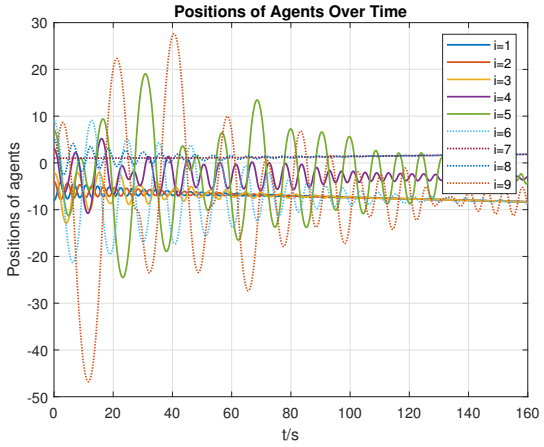

(a) Position

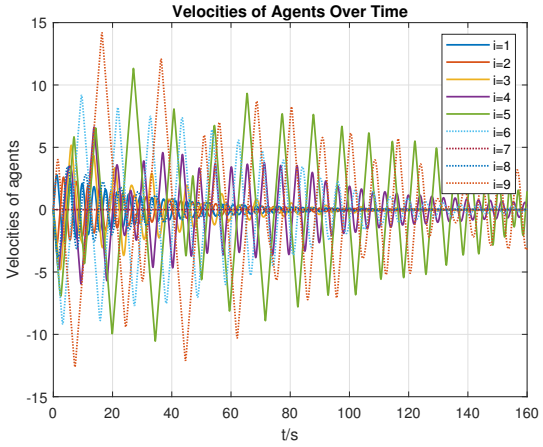

(b) Velocity

Figure 4. Heterogeneous multi-agent systems (HMASs) with a time delay of $\tau = 0.35$ s are analyzed under the topology configuration in Figure 2.

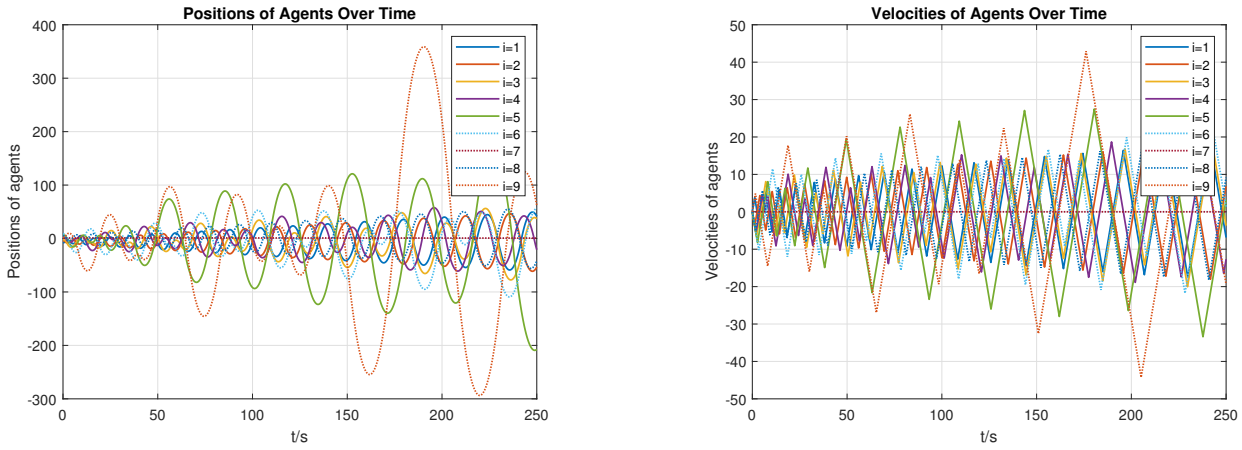

(a) Position **(b)** Velocity

Figure 5. Heterogeneous multi-agent systems (HMASs) with a time delay of $\tau = 0.37$ s are analyzed under the topology configuration in Figure 2.

The simulation results indicate that group consensus (GC) in heterogeneous multi-agent systems (HMASs) is attainable when $\tau < 0.35$ s, but it becomes unattainable when $\tau > 0.35$ s.

Example 4.2. (Undirected Topology)

Consider the HMASs described in Example 4.1, now embedded within an undirected network topology. Figure 6 illustrates the nine-agent configuration. Upon examining Figure 6, key insights can be gleaned.

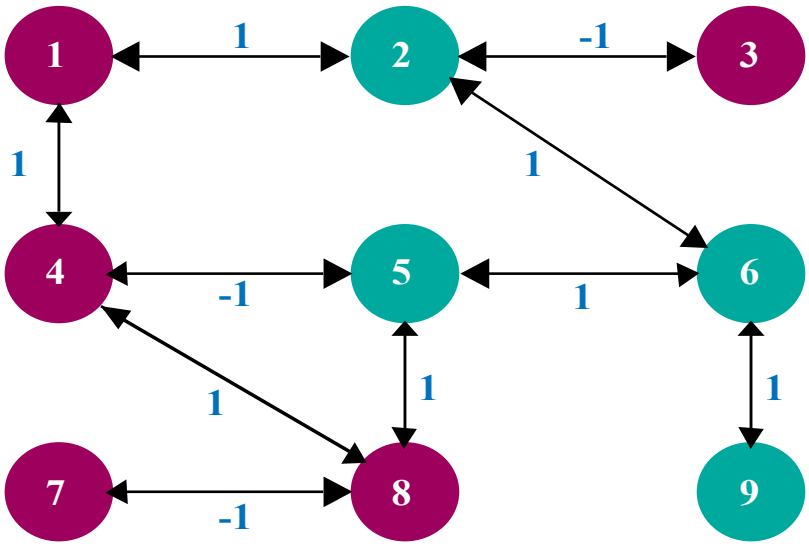

Figure 6. Undirected topology of nine agents.

From Figure 6,

$$\mathcal{D} = \begin{bmatrix} 2 & 0 & 0 & 0 & 0 & 0 & 0 & 0 & 0 \\ 0 & 3 & 0 & 0 & 0 & 0 & 0 & 0 & 0 \\ 0 & 0 & 1 & 0 & 0 & 0 & 0 & 0 & 0 \\ 0 & 0 & 0 & 3 & 0 & 0 & 0 & 0 & 0 \\ 0 & 0 & 0 & 0 & 3 & 0 & 0 & 0 & 0 \\ 0 & 0 & 0 & 0 & 0 & 3 & 0 & 0 & 0 \\ 0 & 0 & 0 & 0 & 0 & 0 & 1 & 0 & 0 \\ 0 & 0 & 0 & 0 & 0 & 0 & 0 & 3 & 0 \\ 0 & 0 & 0 & 0 & 0 & 0 & 0 & 0 & 1 \end{bmatrix} \tag{4.1}$$

$$\mathcal{B} = \begin{bmatrix} 0 & 1 & 0 & 1 & 0 & 0 & 0 & 0 & 0 \\ 1 & 0 & -1 & 0 & 0 & 1 & 0 & 0 & 0 \\ 0 & -1 & 0 & 0 & 0 & 0 & 0 & 0 & 0 \\ 1 & 0 & 0 & 0 & -1 & 0 & 0 & 1 & 0 \\ 0 & 0 & 0 & -1 & 0 & 1 & 0 & 1 & 0 \\ 0 & 1 & 0 & 0 & 1 & 0 & 0 & 0 & 1 \\ 0 & 0 & 0 & 0 & 0 & 0 & 0 & -1 & 0 \\ 0 & 0 & 0 & 1 & 1 & 0 & -1 & 0 & 0 \\ 0 & 0 & 0 & 0 & 0 & 1 & 0 & 0 & 0 \end{bmatrix}$$

The combined matrix $\mathcal{D} + \mathcal{B}$, representing the overall communication topology, is as follows:

$$\mathcal{D} + \mathcal{B} = \begin{bmatrix} 2 & 1 & 0 & 1 & 0 & 0 & 0 & 0 & 0 \\ 1 & 3 & -1 & 0 & 0 & 1 & 0 & 0 & 0 \\ 0 & -1 & 1 & 0 & 0 & 0 & 0 & 0 & 0 \\ 1 & 0 & 0 & 3 & -1 & 0 & 0 & 1 & 0 \\ 0 & 0 & 0 & -1 & 3 & 1 & 0 & 1 & 0 \\ 0 & 1 & 0 & 0 & 1 & 3 & 0 & 0 & 1 \\ 0 & 0 & 0 & 0 & 0 & 0 & 1 & -1 & 0 \\ 0 & 0 & 0 & 1 & 1 & 0 & -1 & 3 & 0 \\ 0 & 0 & 0 & 0 & 0 & 1 & 0 & 0 & 1 \end{bmatrix}$$

The eigenvalues of the combined matrix, $\mathcal{D} + \mathcal{B}$, are calculated as 0, 0.4218, 0.6419, 1.0841, 1.8818, 2.5967, 4.0481, 4.4624, and 4.8632. Consider an HMAS with parameters $\kappa = 3.8$ and $\gamma = 2$, and initial agent states correspond to those in Example 4.1. Theorems 3.1 and 3.4 yield $\tau < 0.13$ s, indicating a global consensus (GC) achievement ability under an undirected topology for input delays below 0.13 s. Simulations with delays $\tau = 0.11$ s, 0.13 s, and 0.15 s produce position and velocity trajectories from Figures 7–9, demonstrating GC feasibility when $\tau < 0.13$ s, but unachievable when $\tau > 0.13$ s. These results demonstrate that as DoS attack severity and disturbances increase, the system's ability to maintain consensus diminishes, highlighting the need for robust communication strategies to ensure stability in HMASs.

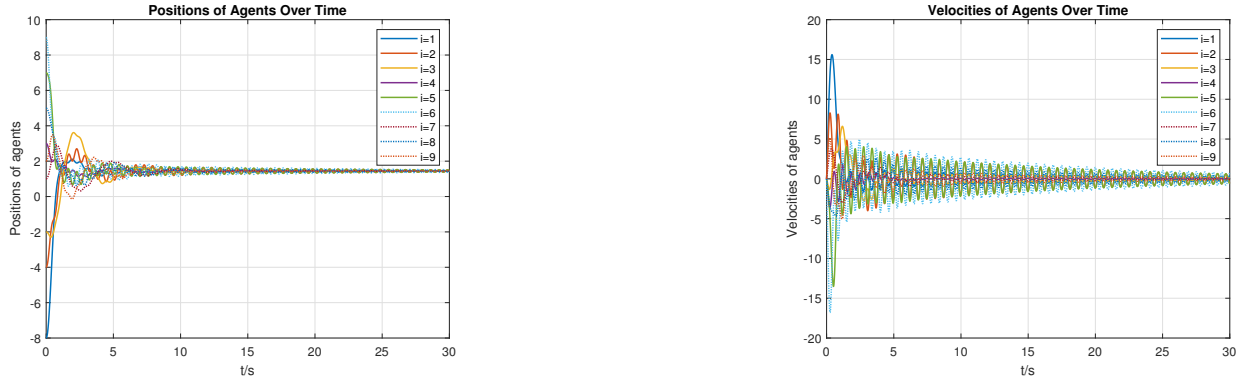

(a) Position **(b)** Velocity

Figure 7. Heterogeneous multi-agent systems (HMASs) with a time delay of $\tau = 0.11$ s are analyzed under the topology configuration in Figure 6.

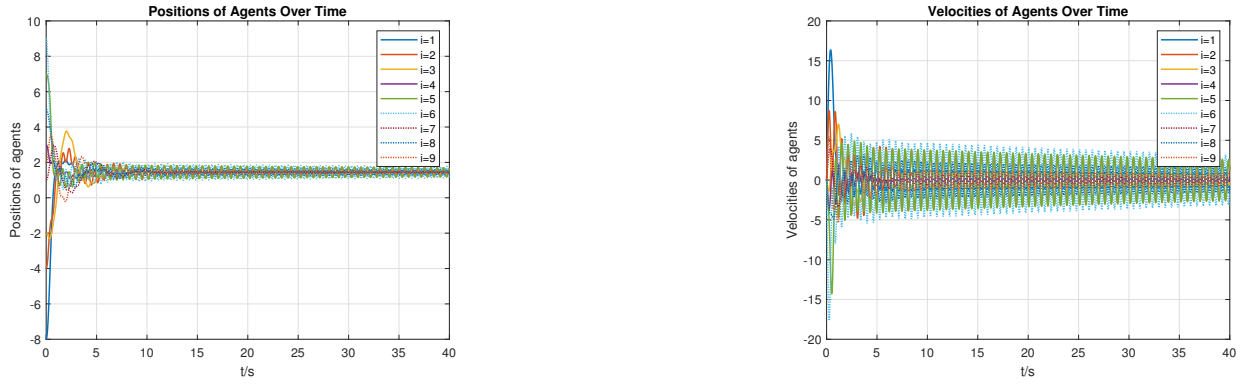

(a) Position **(b)** Velocity

Figure 8. Heterogeneous multi-agent systems (HMASs) with a time delay of $\tau = 0.13$ s are analyzed under the topology configuration in Figure 6.

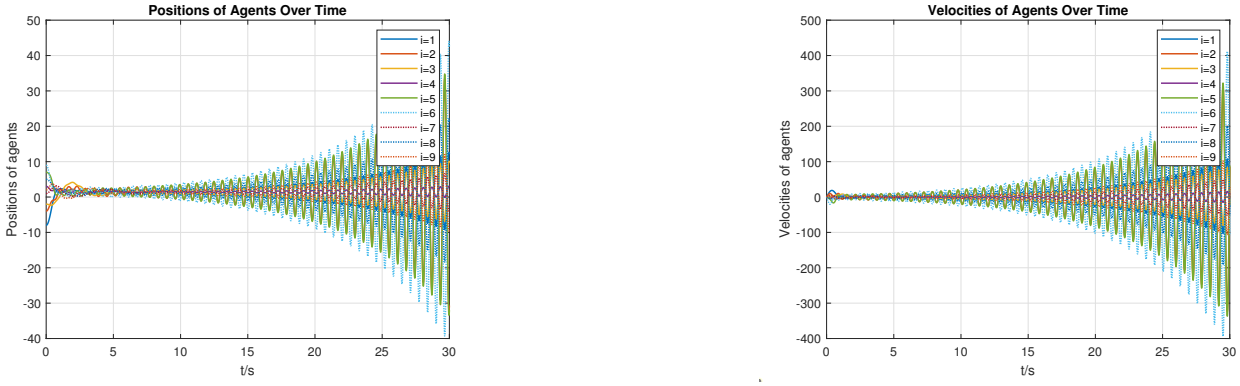

(a) Position **(b)** Velocity

Figure 9. Heterogeneous multi-agent systems (HMASs) with a time delay of $\tau = 0.15$ s are analyzed under the topology configuration in Figure 6.

The proposed control protocol is compared with existing approaches in Table 1, highlighting its advantages in handling mixed-order agents, delays, denial of service (DoS) attacks, and disturbances while achieving consensus. Unlike prior works that address these challenges in isolation, our method integrates all four factors, as demonstrated in the simulations. For instance, the proposed protocol achieves consensus across both directed and undirected network topologies, even when input delays approach critical limits. This level of robustness, which is not addressed in the compared studies, highlights the practical applicability of the framework in real-world HMAS scenarios.

Table 1. Concise comparison of related works.

Ref.	Topic	Mixed-Order	Delay	DoS	Disturbance	Consensus (HMAS)
[37]	Containment control (NN-based, homogeneous agents)	✗	✗	✗	✗	✗
[38]	Game-theoretic regret minimization	✗	✗	✗	✗	✗
[39]	Neural network synchronization (single-system)	✗	✓	✗	✗	✗
[40]	PIR control for single-agent systems	✗	✓	✗	✓	✗
[41]	Delay analysis (CTCR)	✗	✓	✗	✗	✗
[42]	Event-triggered control (HiTL)	✗	✗	✗	✓	✗
[43]	Nonlinear consensus with UIO	✗	✗	✗	✓	✗
Ours	Robust consensus under delay, DoS, and disturbance	✓	✓	✓	✓	✓

Practical implications and comparative discussion

The simulation results demonstrate that heterogeneous multi-agent systems (HMASs) are notably sensitive to input delays, particularly under denial of service (DoS) attacks and external disturbances. When the input delay remains below a critical threshold—such as 0.35 seconds for the directed topology and 0.13 seconds for the undirected topology—the system consistently reaches group consensus. However, when the delay exceeds these bounds, system instability arises and coordination among agents fails.

These observations have direct implications for practical applications. For instance, in autonomous vehicle networks, communication interruptions caused by DoS attacks can lead to coordination breakdowns. Similarly, in cooperative robotics and distributed sensor platforms, input delays and environmental disturbances can compromise system reliability and performance.

The control protocol presented in this work, which integrates competitive and cooperative

interactions among mixed-order agents, performs robustly even under such adverse conditions. Unlike previous studies that often assume homogeneous dynamics or ignore the joint effects of input delay and attack patterns, the proposed approach provides algebraic delay bounds based on system structure and eigenvalue analysis. This not only improves resilience but also offers a systematic method for anticipating critical thresholds without relying on exhaustive testing.

Table 2 summarizes the observed relationship between input delay and group consensus under both topologies considered in the simulations:

Table 2. Comparative analysis of delay thresholds under different topologies.

Topology	**Delay (τ)**	**Consensus**	**System Behavior**
Directed	0.33 s	Yes	Stable coordination
Directed	0.35 s	Borderline	Slower convergence
Directed	0.37 s	No	Divergence observed
Undirected	0.11 s	Yes	Smooth group consensus
Undirected	0.13 s	Borderline	Acceptable performance
Undirected	0.15 s	No	Rapid instability

These findings emphasize the need for delay-aware and disturbance-resilient control strategies when designing HMASs for real-world systems. By quantifying the relationship between delay tolerance and system dynamics, the proposed framework offers a practical guideline for achieving reliable coordination in uncertain or disrupted environments.

5. Conclusions

This paper proposes a robust group consensus protocol for heterogeneous multi-agent systems (HMASs) operating under the combined effects of input delays, external disturbances, and denial of service (DoS) attacks. The design accommodates both cooperative and competitive relationships among agents and incorporates virtual velocity states to support consensus under intermittent communication and dynamic challenges. The approach is particularly relevant to practical systems such as autonomous vehicle networks, smart grid infrastructures, and industrial automation, where maintaining coordinated behavior despite disruptions is essential.

A frequency-domain framework is employed to derive algebraic conditions that relate control parameters, delay bounds, and the dominant eigenvalue of the system matrix. The theoretical findings are validated through numerical simulations, confirming the protocol's ability to preserve group coordination even in the presence of cyber-induced interruptions. The protocol also supports flexible network configurations, allowing intra-subgroup communication without reliance on bipartite graph structures. Additionally, it is applicable to both directed and undirected topologies, which broadens its practical relevance and addresses key limitations found in earlier consensus models.

It is also important to note that the delay bound derived in this study represents a conservative estimate based on the proposed control formulation. While it provides a sufficient condition for system stability, it does not represent the exact limit of stability margins. As a future direction, more refined frequency-domain techniques—such as the analysis of imaginary spectra in the domain of multiple time delays—may be adopted to derive precise stability boundaries. Moreover, future work

may explore extensions to time-varying or switching topologies and incorporate distributed or proportional delay models, further enhancing the applicability of the proposed protocol in real-world multi-agent systems.

Author contributions

A. B. Rajab: Conceptualization; A. Khan and M. M. A. Almazah: Software, resources; T. Saidani: Validation; A. Khan and M. A. Javeed: Formal analysis; R. Ashfaq: Data curation; R. Ashfaq and A. U. K. Niazi: Writing – original draft, writing – review & editing; A. U. K. Niazi and Y. B. Zhong: Supervision; Y. B. Zhong and A. Khan: Project administration. All authors have read and approved the final version of the manuscript for publication.

Use of Generative-AI tools declaration

The authors declare they have not used Artificial Intelligence (AI) tools in the creation of this article.

Acknowledgments

This research was sponsored by the Deanship of Research and Graduate Studies at King Khalid University through the Large Research Project under grant number RGP.2/70/46, the National Natural Science Foundation of China grant No. 12250410247, the Ministry of Science and Technology of China, grant No. WGXZ2023054L, and the Deanship of Scientific Research at Northern Border University, Arar, KSA, through project number NBU-CRP-2025-2225.

Conflict of interest

The authors declare that they have no conflict of interest.

References

1. F. Yu, L. Ji, S. Yang, Group consensus for a class of heterogeneous multi-agent networks in the competition systems, *Neurocomputing*, **416** (2020), 165–171. https://doi.org/10.1016/j.knosys.2023.111358
2. D. Pang, H. Meng, J. Cao, S. Liu, Group consensus protocol with input delay for HMASs in cooperative-competitive networks, *Neurocomputing*, **596** (2024), 127931. https://doi.org/10.1016/j.neucom.2024.127931
3. Y. Lan, J. Zhao, Improving track performance by combining Padé-approximation-based preview repetitive control and equivalent-input-disturbance, *J. Electr. Eng. Technol.*, **19** (2024), 3781–3794. https://doi.org/10.1007/s42835-024-01830-x
4. Q. Ma, S. Xu, Intentional delay can benefit consensus of second-order multi-agent systems, *Automatica*, **147** (2023), 110750. https://doi.org/10.1016/j.automatica.2022.110750

5. F. Ding, K. Zhu, J. Liu, C. Peng, Y. Wang, J. Lu, Adaptive memory event triggered output feedback finite-time lane keeping control for autonomous heavy truck with roll prevention, *IEEE T. Fuzzy Syst.*, **32** (2024), 6607–6621. https://doi.org/10.1109/TFUZZ.2024.3454344

6. J. Chen, J. Wang, J. Wang, L. Bai, Joint fairness and efficiency optimization for CSMA/CA-based multi-user MIMO UAV Ad Hoc networks, *IEEE J. STSP*, **18** (2024), 1311–1323. https://doi.org/10.1109/JSTSP.2024.3435348

7. L. Ji, Z. Lin, C. Zhang, S. Yang, J. Li, H. Li, Data-based optimal consensus control for multiagent systems with time delays: Using prioritized experience replay, *IEEE T. Syst. Man Cy.-S.*, **54** (2024), 3244–3256. https://doi.org/10.1109/TSMC.2024.3358293

8. S. Jin, X. Wang, Q. Meng, Spatial memory-augmented visual navigation based on hierarchical deep reinforcement learning in unknown environments, *Knowl.-Based Syst.*, **285** (2024), 111358. https://doi.org/10.1016/j.knosys.2023.111358

9. Y. Yao, F. Shu, X. Cheng, H. Liu, P. Miao, L. Wu, Automotive radar optimization design in a spectrally crowded V2I communication environment, *IEEE T. Intell. Transp. Sy.*, **24** (2023), 8253–8263. https://doi.org/10.1109/TITS.2023.3264507

10. J. Shi, C. Liu, J. Liu, Hypergraph-based model for modelling multi-agent q-learning dynamics in public goods games, *IEEE T. Netw. Sci. Eng.*, **11** (2024), 6169–6179. https://doi.org/10.1109/TNSE.2024.3473941

11. X. Wu, B. Zou, C. Lu, L. Wang, Y. Zhang, H. Wang, Dynamic security computing framework with zero trust based on privacy domain prevention and control theory, *IEEE J. Sel. Area. Commun.*, **43** (2025), 2266–2278. https://doi.org/10.1109/JSAC.2025.3560036

12. X. Peng, S. Song, X. Zhang, M. Dong, K. Ota, Task offloading for IoAV under extreme weather conditions using dynamic price driven double broad reinforcement learning, *IEEE Internet Things*, **11** (2024), 17021–17033. https://doi.org/10.1109/JIOT.2024.3360110

13. Z. Zhou, Y. Wang, G. Zhou, K. Nam, Z. Ji, C. Yin, A twisted Gaussian risk model considering target vehicle longitudinal-lateral motion states for host vehicle trajectory planning, *IEEE T. Intell. Transp.*, **24** (2023), 13685–13697. https://doi.org/10.1109/TITS.2023.3298110

14. Z. Li, J. Hu, B. Leng, L. Xiong, Z. Fu, An integrated of decision making and motion planning framework for enhanced oscillation-free capability, *IEEE T. Intell. Transp.*, **25** (2024), 5718–5732. https://doi.org/10.1109/TITS.2023.3332655

15. F. Wang, K. Chen, S. Zhen, X. Chen, H. Zheng, Z. Wang, Prescribed performance adaptive robust control for robotic manipulators with fuzzy uncertainty, *IEEE Trans. Fuzzy Syst.*, **32** (2024), 1318–1330. https://doi.org/10.1109/TFUZZ.2023.3323090

16. H. Xu, H. Wei, H. Chen, Z. Chen, X. Zhou, H. Xu, et al., Effect of periodic phase modulation on the matched filtering with insufficient phase shift capability, *IEEE T. Aero. Elec. Sys.*, **61** (2025), 5755–5770. https://doi.org/10.1109/TAES.2024.3520959

17. G. Du, H. Zhang, H. Yu, P. Hou, J. He, S. Cao, et al., Study on automatic tracking system of microwave deicing device for railway contact wire, *IEEE T. Instrum.*, **73** (2024), 1–11. https://doi.org/10.1109/TIM.2024.3446638

18. Y. Cao, Z. Zhang, Enhanced contour tracking: A time-varying internal model principle-based approach, *IEEE-ASME T. Mech.*, 2025, 1–9. https://doi.org/10.1109/TMECH.2025.3572743

19. H. Zhang, Y. Xu, R. Luo, Y. Mao, Fast GNSS acquisition algorithm based on SFFT with high noise immunity, *China Commun.*, **20** (2023), 70–83. https://doi.org/10.23919/JCC.2023.00.006

20. Z. Zhao, X. Chen, F. Meng, Z. Yang, B. Liu, N. Zhu, et al., Design and analysis of a 22.6-to-73.9 GHz low-noise amplifier for 5G NR FR2 and NR-U multiband/multistandard communications, *IEEE J. Solid-St. Circ.*, 2025, 1–13. https://doi.org/10.1109/JSSC.2025.3545463

21. X. Yang, Y. Zhuang, M. Shi, X. Sun, X. Cao, B. Zhou, RatioVLP: Ambient light noise evaluation and suppression in the visible light positioning system, *IEEE T. Mobile Comput.*, **23** (2024), 5755–5769. https://doi.org/10.1109/TMC.2023.3312550

22. J. Wu, Y. Wang, C. Yin, Curvilinear multilane merging and platooning with bounded control in curved road coordinates, *IEEE T. Veh. Technol.*, **71** (2022), 1237–1252. https://doi.org/10.1109/TVT.2021.3131751

23. X. Zhang, Y. Liu, X. Chen, Z. Li, C. Su, Adaptive pseudoinverse control for constrained hysteretic nonlinear systems and its application on dielectric elastomer actuator, *IEEE-ASME T. Mech.*, **28** (2023), 2142–2154. https://doi.org/10.1109/TMECH.2022.3231263

24. J. Lv, X. Ju, C. Wang, Neural network prescribed-time observer-based output-feedback control for uncertain pure-feedback nonlinear systems, *Expert Syst. Appl.*, **264** (2025), 125813. https://doi.org/10.1016/j.eswa.2024.125813

25. X. Ju, Y. Jiang, L. Jing, P. Liu, Quantized predefined-time control for heavy-lift launch vehicles under actuator faults and rate gyro malfunctions, *ISA T.*, **138** (2023), 133–150. https://doi.org/10.1016/j.isatra.2023.02.022

26. Y. Liu, Q. Hu, G. Feng, Navigation functions on 3-manifold with boundary as a disjoint union of Hopf tori, *IEEE T. Automat. Contr.*, **70** (2025), 219–234. https://doi.org/10.1109/TAC.2024.3419817

27. H. Liu, S. Zhen, X. Liu, H. Zheng, L. Gao, Y. Chen, Robust approximate constraint following control design for collaborative robots system and experimental validation, *Robotica*, **42** (2024), 3957–3975. https://doi.org/10.1017/S0263574724001760

28. Y. Liu, W. Li, X. Dong, Z. Ren, Resilient formation tracking for networked swarm systems under malicious data deception attacks, *Int. J. Robust Nonlin.*, **35** (2025), 2043–2052. https://doi.org/10.1002/rnc.7777

29. Y. Lan, J. Zhao, Improving track performance by combining Padé-approximation-based preview repetitive control and equivalent-input-disturbance, *J. Electr. Eng. Technol.*, **19** (2024), 3781–3794. https://doi.org/10.1007/s42835-024-01830-x

30. R. Yang, S. Liu, X. Li, Observer-based bipartite containment control of fractional multi-agent systems with mixed delays, *Inform. Sci.*, **626** (2023), 204–222. https://doi.org/10.1016/j.ins.2023.01.025

31. Y. Zhang, Y. Hong, M. Guizani, S. Wu, P. Zhang, R. Liu, A multi-layer information dissemination model and interference optimization strategy for communication networks in disaster areas, *IEEE T. Veh. Technol.*, **73** (2024), 1239–1252. https://doi.org/10.1109/TVT.2023.3304707

32. X. Li, Z. Lu, M. Yuan, W. Liu, F. Wang, Y. Yu, et al., Tradeoff of code estimation error rate and terminal gain in SCER attack, *IEEE T. Instrum. Meas.*, **73** (2024), 1–12. https://doi.org/10.1109/TIM.2024.3406807
33. W. Wang, J. Liang, H. Zeng, Sampled-data-based stability and stabilization of Lurie systems, *Appl. Math. Comput.*, **501** (2025), 129455. https://doi.org/10.1016/j.amc.2025.129455
34. W. Wang, C. Li, A. Luo, H. Xiao, Stability analysis of linear systems with a periodical time-varying delay based on an improved non-continuous piecewise Lyapunov functional, *AIMS Math.*, **10** (2025), 9073–9093. https://doi.org/10.3934/math.2025418
35. Z. Liu, G. Jiang, Y. Wu, T. Wang, S. Liu, Z. Ouyang, K-coverage estimation for irregular targets in wireless visual sensor networks deployed in complex region of interest, *IEEE Sens. J.*, **25** (2025), 18370–18383. https://doi.org/10.1109/JSEN.2025.3558041
36. F. Xu, H. Yang, M. Alouini, Energy consumption minimization for data collection from wirelessly-powered IoT sensors: Session-specific optimal design with DRL, *IEEE Sens. J.*, **22** (2022), 19886–19896. https://doi.org/10.1109/JSEN.2022.3205017
37. X. Wang, N. Pang, Y. Xu, T. Huang, J. Kurths, On state-constrained containment control for nonlinear multiagent systems using event-triggered input, *IEEE T. Syst. Man Cy.-S.*, **54** (2024), 2530–2538. https://doi.org/10.1109/TSMC.2023.3345365
38. Z. Wang, C. Mu, S. Hu, C. Chu, X. Li, Modelling the dynamics of regret minimization in large agent populations: A master equation approach, In: *Proceedings of the Thirty-First International Joint Conference on Artificial Intelligence (IJCAI-22)*, 2022, 534–540. https://doi.org/10.24963/ijcai.2022/76
39. Y. Wang, Q. Song, Y. Liu, Synchronisation of quaternion-valued neural networks with neutral delay and discrete delay via aperiodic intermittent control, *Int. J. Syst. Sci.*, **56** (2025), 1395–1412. https://doi.org/10.1080/00207721.2024.2427249
40. X. Zhang, Q. Gao, J. Cai, W. Xu, Design and comprehensive analysis of improved Proportional-Integral-Retarded protocol for second-order multi-agent systems, *Inform. Sci.*, **666** (2024), 120396. https://doi.org/10.1016/j.ins.2024.120396
41. Q. Gao, J. Cai, R. Cepeda-Gomez, W. Xu, Improved frequency sweeping technique and stability analysis of the second-order consensus protocol with distributed delays, *Int. J. Control*, **96** (2023), 461–474. https://doi.org/10.1080/00207179.2021.2002415
42. L. Ma, F. Zhu, Human-in-the-loop formation control for multi-agent systems with asynchronous edge-based event-triggered communications, *Automatica*, **167** (2024), 111744. https://doi.org/10.1016/j.automatica.2024.111744
43. F. Zhu, Y. Zhao, Y. Fu, T. N. Dinh, Observer-based output consensus control scheme for strict-feedback nonlinear multi-agent systems with disturbances, *IEEE T. Netw. Sci. Eng.*, **11** (2023), 2621–2631. https://doi.org/10.1109/TNSE.2023.3346442

AIMS Press